Applied Geography 87 (2017) 14–27

Contents lists available at ScienceDirect

Applied Geography

journal homepage: www.elsevier.com/locate/apgeog

Using reverse geocoding to identify prominent wildfire evacuation trigger points

Dapeng Li [a, *], Thomas J. Cova [b], Philip E. Dennison [b]

[a] Department of Geography, South Dakota State University, 109 Wecota Hall, Box 506, Brookings, SD 57007, USA
[b] Center for Natural and Technological Hazards (CNTH), Department of Geography, University of Utah, 332 S 1400 E, RM. 217, Salt Lake City, UT, 84112, USA

ARTICLE INFO

Article history:
Received 22 September 2016
Received in revised form
20 May 2017
Accepted 23 May 2017
Available online 1 August 2017

Keywords:
Wildfire evacuation
Evacuation timing
Trigger modeling
Reverse geocoding
Fire spread modeling
Viewshed analysis

ABSTRACT

Wildfire evacuation trigger points are prominent geographic features (e.g., ridge lines, rivers, and roads) utilized in timing evacuation warnings. When a fire crosses a feature, an evacuation warning is issued to the communities or firefighters in the path of the fire. Current methods for generating trigger buffers have limited utility because the resulting buffers are not explicitly tied to prominent geographic features, making it difficult to visually determine when a fire has breached a trigger point. This work aims to address this limitation by using reverse geocoding to identify prominent geographic trigger points that have more value to emergency managers. The method consists of three steps: 1) generate a trigger buffer using fire-spread modeling; 2) utilize online reverse-geocoding to retrieve geographic features proximal to the buffer boundary; and 3) identify the most prominent geographic features using viewshed analysis and compute the warning time each would offer given predicted fire spread rates to proximal communities. A case study of Julian, California is presented to identify prominent geographic trigger points that may have value to emergency managers in improving the timing of wildfire evacuation warnings in this region.

1. Introduction

The wildland urban interface (WUI) is defined as the area where urban settings and wildlands meet (Radeloff et al., 2005; Stewart, Radeloff, Hammer, & Hawbaker, 2007). Many people move to the WUI for rural amenities (Davis, 1990), and the past few decades have witnessed rapid WUI population growth in the American West (Hammer, Stewart, & Radeloff, 2009; Theobald & Romme, 2007). At the same time, wildfire occurrence and total area burned have increased, which corresponds with an increase in drought severity in many regions (Dennison, Brewer, Arnold, & Moritz, 2014). Wildfires pose a significant threat to WUI residents, and improving public safety in these areas has received considerable research attention (Brenkert–Smith, Champ, & Flores, 2006; Cova, Dennison, & Drews, 2011; Mell, Manzello, Maranghides, Butry, & Rehm, 2010).

When an advancing fire becomes a threat to the residents of a community, protective actions may need to be recommended to ensure public safety. Common protective actions in wildfires include evacuation and shelter-in-place (SIP) (Cova, Drews, Siebeneck, & Musters, 2009). When threatened residents have enough time to evacuate to safer places, incident commanders (ICs) tend to recommend this option to maximize public safety, but when a fire advances too fast and the residents do not have enough time for evacuation, SIP may be recommended so that the residents will not be trapped in transit (Cova et al., 2011). To aid in timing protective action recommendations (PARs), prominent geographic features (e.g., ridge lines, rivers, and roads) may be used as triggers, such that when a fire crosses a feature, a PAR will be issued to the threatened residents or firefighters in the fire's path (Cook, 2003; Cova, Dennison, Kim, & Moritz, 2005). A key characteristic of effective trigger points is *prominence*, as it improves the chance that a triggering event will be readily detected by decision makers.

Existing wildfire trigger research relies on fire-spread modeling and geographic information systems (GIS) to model and set triggers (Cova et al., 2005). Fire-spread models simulate the spread of fire over time and space from an ignition point. In trigger modeling, fire spread modeling can be reversed to model the spread of fire from

* Corresponding author. Department of Geography, South Dakota State University, 109 Wecota Hall, Box 506, Brookings, SD 57007, USA.
E-mail addresses: lidapeng85@gmail.com (D. Li), cova@geog.utah.edu (T.J. Cova), dennison@geog.utah.edu (P.E. Dennison).

http://dx.doi.org/10.1016/j.apgeog.2017.05.008
0143-6228/

the threatened geographic assets outwards to generate a trigger buffer given an estimated evacuation time. Initial work has been conducted to examine the sensitivity of trigger modeling with varying weather inputs (Fryer, Dennison, & Cova, 2013; Larsen, Dennison, Cova, & Jones, 2011). In general, these triggers have been polygons, lines, or points that do not correspond to prominent geographic features (Dennison, Cova, & Moritz, 2007). Reverse geocoding, the process of identifying geographic features from coordinates, has the potential to associate prominent features with the boundary of trigger buffers. The goal of this paper is to present a new method for identifying prominent geographic trigger points that may have more value to emergency managers in providing a minimum amount of warning time.

2. Background

2.1. Trigger modeling

Current trigger modeling methods employ fire-spread modeling and GIS to create a raster trigger buffer around a threatened geographic asset (Cova et al., 2005) using a three-step process (Dennison et al., 2007). In the first step, the fire spread modeling software FlamMap is employed to calculate fire spread rates within a raster cell in eight directions under varying assumptions regarding fuel, wind, and humidity. Note that the fire spread rates derived from FlamMap (Finney, 2006) are based on the Rothermel model (Rothermel, 1972). The second step constructs a fire-spread network by connecting the centroids of orthogonally and diagonally adjacent raster cells to represent fire travel times between adjacent cells. In the third step, the travel times between two adjacent cells are reversed, and the Dijkstra shortest path algorithm (Dijkstra, 1959) is employed to traverse the graph from the input raster feature outwards until the accumulated travel time reaches the input time constraint. The output of trigger modeling is a raster trigger buffer around the threatened asset for a specific input time (e.g., estimated evacuation time). Previous studies have demonstrated that trigger modeling may have potential in a variety of applications, e.g., protecting firefighters (Cova et al., 2005; Fryer et al., 2013), planning community evacuations (Dennison et al., 2007; Larsen et al., 2011), protecting pedestrians in wildlands (Anguelova, Stow, Kaiser, Dennison, & Cova, 2010), and issuing household-level evacuation warnings (Li, Cova, & Dennison, 2015).

2.2. Geocoding and reverse geocoding

Geocoding refers to the process of assigning geographic coordinates to addresses or place names (Goldberg, Wilson, & Knoblock, 2007). Geocoding has been widely used in applications such as public health (Krieger, 1992; Krieger et al., 2002; Rushton et al., 2006), crime (Andresen, 2006; Ratcliffe, 2004), and traffic accident analysis (Lascala, Gerber, & Gruenewald, 2000; Loo, 2006). Geocoding quality and its impacts on spatial analysis have attracted substantial research attention (Bonner et al., 2003; Zandbergen, 2009, 2011; Zandbergen, Hart, Lenzer, & Camponovo, 2012). Reverse geocoding is a process that associates geographic features with geographic coordinates (Kounadi, Lampoltshammer, Leitner, & Heistracher, 2013). Existing studies on reverse geocoding focus on privacy issues (Kounadi et al., 2013; Krumm, 2007). Geocoding and reverse geocoding can be done with installed software or using on-line services. A number of studies have been conducted to evaluate the quality of online geocoding services (Karimi, Sharker, & Roongpiboonsopit, 2011; Roongpiboonsopit & Karimi, 2010). These studies employed the same metrics in evaluating offline geocoding quality to assess the quality of online geocoding services. Existing research on online reverse geocoding usually focuses on the accuracy of these services in urban areas (McKenzie & Janowicz, 2015). For example, a study by Kounadi et al. (2013) examined the accuracy and privacy issues of using different online reverse geocoding services in crime studies.

2.3. Feature prominence

The problem of identifying prominent geographic features appears in a variety of applications, such as wilderness landmark-based navigation and search and rescue (SAR) (Duckham, Kulik, & Worboys, 2003; Millonig & Schechtner, 2007; Zhu & Karimi, 2015). One issue related to the value of using derived features as trigger points is prominence, which refers to the degree to which a feature can be identified from its surrounding environment. A prominent feature can be used by nearby firefighters for communication and navigation purposes during wildfire evacuations. Viewshed analysis has been used as one means to evaluate feature visibility (Fisher, 1993). A typical viewshed analysis procedure takes a digital elevation model (DEM) and a viewpoint as the input and calculates whether a line-of-sight (LoS) can reach each raster cell in the landscape. A cumulative viewshed uses multiple viewing points to compute how many times a point in the landscape can be visible from these viewpoints (Fisher, Farrelly, Maddocks, & Ruggles, 1997). However, many factors can influence the visibility of a feature, e.g., weather conditions and natural or man-made obstructions (Llobera, 2003). Thus, a positive result from viewshed analysis may not guarantee that a feature is visible from the viewpoint in all cases.

3. Methods

Fig. 1 presents a three-step method that integrates trigger modeling, reverse geocoding, and a computational means for measuring geographic feature prominence. The following subsections describe each step in more detail.

3.1. Step 1: trigger modeling

In the first step, trigger modeling is performed to create buffers around the geographic location where the threatened population or assets are located (Dennison et al., 2007). This method is based on the raster data model, and the input data can be categorized into five groups: land cover data (fuel types and canopy cover), topographic data (DEM, slope, and aspect), weather inputs (moisture, wind speed, and wind direction), threatened locations (firefighter crew, community, road, house, etc.), and estimated evacuation times. Fig. 2 outlines the three-step process of trigger modeling. In the first step, all the input data are imported into FlamMap, and fire spread modeling is performed to derive fire spread rates in eight directions for each raster cell (Fig. 2(a)). The second step uses the spread rates to compute the travel times between the centroids of orthogonally and diagonally adjacent raster cells to construct a fire travel-time graph. As shown in Fig. 2(b), the centroids of the raster cells are the nodes, and the weights for the arcs are the travel times. The arcs are bi-directional because fire spread rates within one raster cell differ in each direction due to wind, fuel, and topography. In the third step, the directional arcs derived in the second step are reversed, and the Dijkstra (1959) shortest path algorithm is used to traverse from the input location cells until the accumulated travel time reaches the input time. This process is illustrated in Fig. 2(c), which shows the resulting raster trigger buffer.

3.2. Step 2: reverse geocoding

Online reverse geocoding services take one pair of geographic

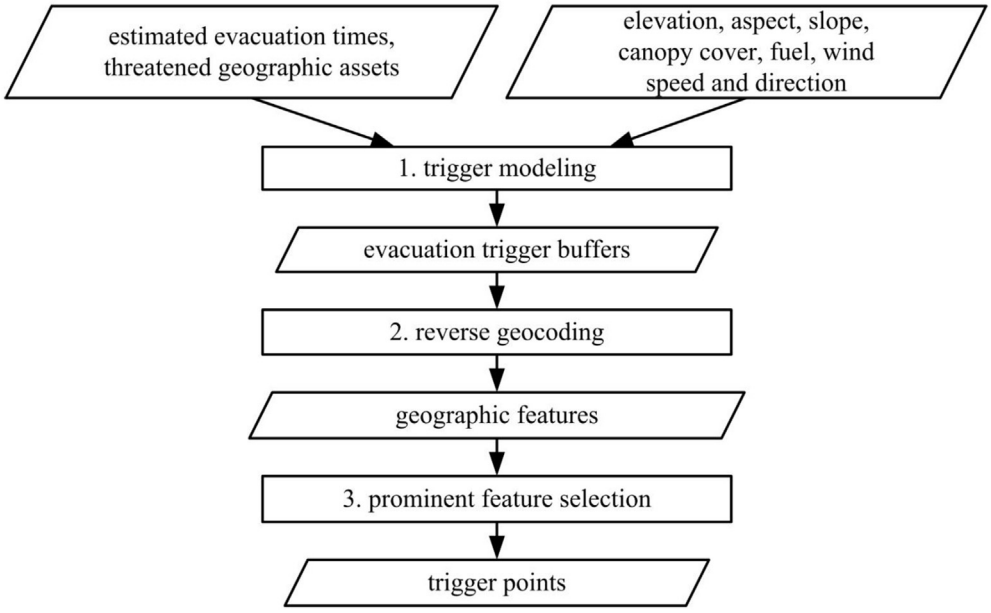

Fig. 1. Workflow of the three-step method.

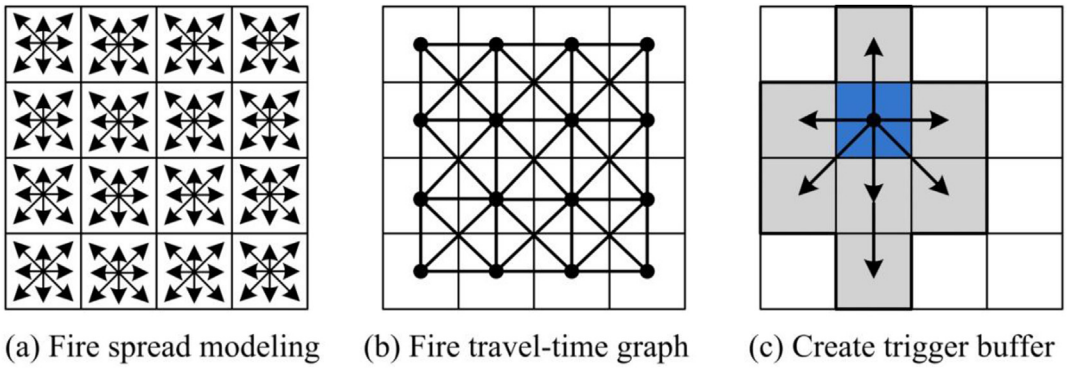

Fig. 2. The three-step trigger modeling process.

coordinates (latitude and longitude) as the input, whereby they return a feature name as well as its location as the output. However, in many real-world applications the input can be other geometries instead of simple points, e.g., line and polygon features. These complex features must be split into points before they can be processed by online reverse geocoding services. In the context of trigger buffer modeling, the centroids of the boundary cells are the vertices, while orthogonally adjacent cells are connected by edges. A boundary cell is defined as a cell in the evacuation trigger buffer (ETB) that has at least one neighbor that does not fall within the ETB. As shown in Fig. 3(a), the blue cells are inside cells, while the gray ones boundary cells. Fig. 3(b) shows the graph representation of the boundary cells. We need to use the buffer boundary as the input to the reverse geocoding process to identify proximal geographic features. Specifically, the centroids of the boundary cells are extracted, and these points are then used as the input for reverse geocoding. An algorithm for extracting the query points and constructing the graph is given in Table 1. A graph is constructed using the boundary query points based on spatial adjacency between boundary cells, and depth first search (DFS) is used to traverse the graph from the top left cell in a clockwise manner, as shown in Fig. 3(c). The graph traversal algorithm can transform the boundary to a linear sequence of cells. Since feature density of online reverse geocoding services in exurban areas is usually low, we could sample the boundary cells at a certain interval to reduce computational load in reverse geocoding.

3.3. Step 3: prominent feature selection

In the prominent feature selection process, we need to take into account both the warning time the feature might offer and its prominence. Fig. 4 depicts these two dimensions where the x axis depicts the feature's prominence, while the y axis depicts the warning time derived from trigger modeling. A feature which falls between the minimum and maximum evacuation time estimates (ETEs) and provides a lead time closer to the most probable ETE would score highly as a more effective trigger point. The other dimension concerns feature prominence, and more prominent features can help a fire scout detect when the fire crosses a feature and communicate this information to an incident commander.

The generated trigger buffer is usually a complex shape due to spatial variability in the input data (e.g., topography and fuel type). Previous studies on trigger modeling have revealed that the size and shape of trigger buffers depend on the inputs such as wind speed and direction (Dennison et al., 2007; Larsen et al., 2011). In reverse geocoding, Euclidean distance has been widely used as a

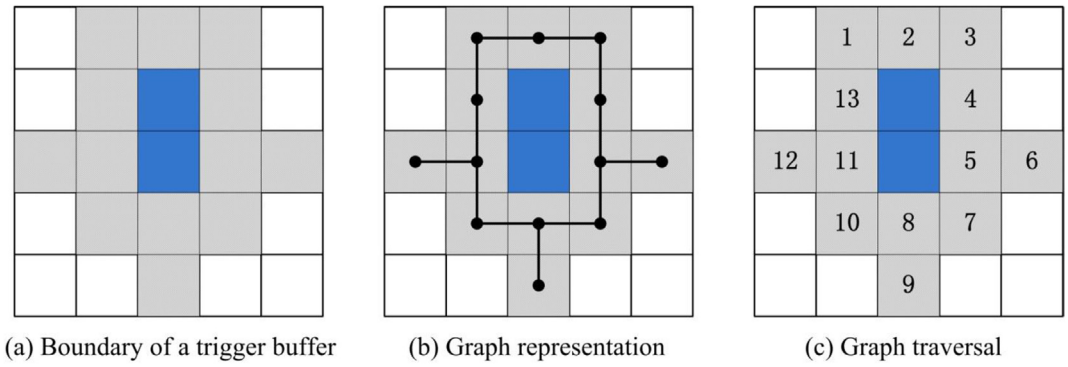

Fig. 3. Illustration of boundary cells and the graph representation.

Table 1
Algorithm for extracting query points from an ETB.

```
1   G = (V, E)                                        // a graph for storing boundary cells
2   ETB = readData( )                                 // read data and ETB is a N by N array
3   For i From 0 To N-1                               // iterate each row
4       For j From 0 To N-1                           // iterate each column
5           If isBoundaryCell(ETB(i, j) ) Is True     // if the cell is a boundary cell
6               G.addVertex(ETB(i, j))                // add the cell to the vertex list
7               For neighbor In ETB(i, j).getNeighbors( ) // for each neighbor cell of ETB(i, j)
8                   If isBoundaryCell(neighbor) Is True   // if it is a boundary cell
9                       G.addVertex(neighbor)             // add it to the vertex list
10                      G.addEdge(ETB(i, j), neighbor)    // add the edge to the edge list
11                      G.addEdge(neighbor, ETB(i, j))    // add the edge to the edge list
12                  EndIf
13              EndFor
14          EndIf
15      EndFor
16  EndFor
```

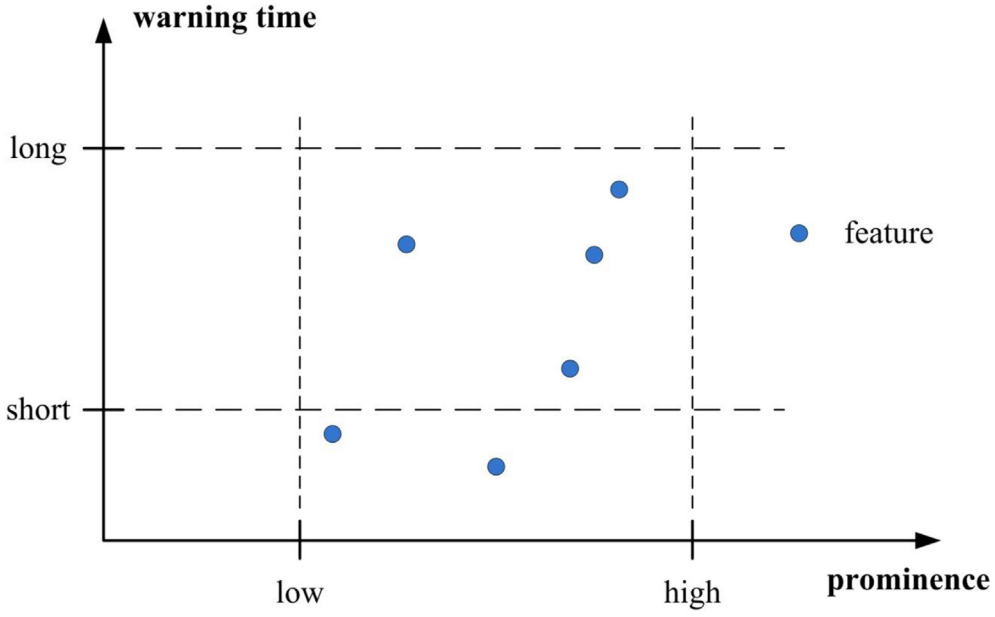

Fig. 4. Two dimensions for prominent feature selection.

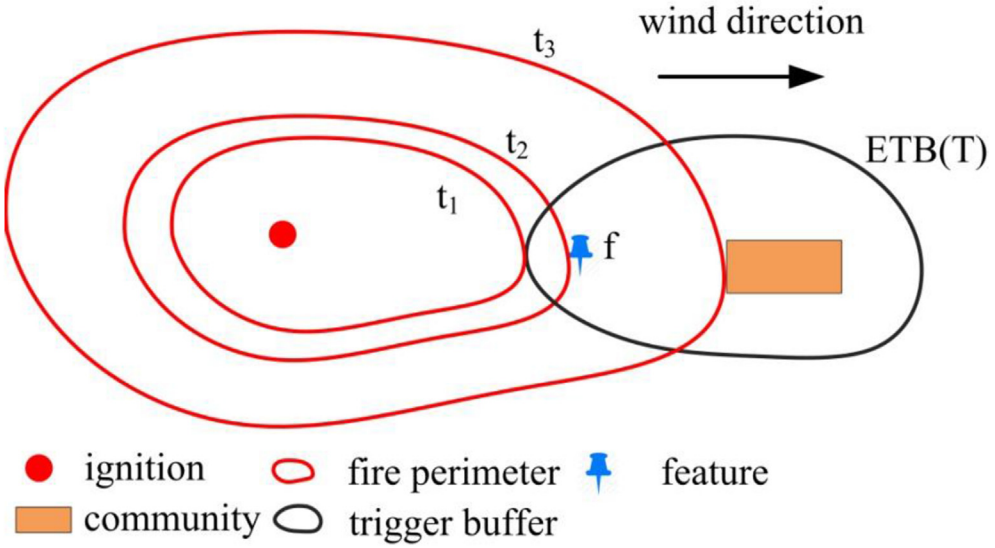

Fig. 5. A conceptual diagram for the timing of warning.

metric to measure the closeness of a returned feature to the input location point. However, the skewedness of trigger buffers makes it inappropriate to use Euclidean distance to measure community risk. In order to solve this issue and facilitate evacuation timing, wildfire spread simulation is employed to compute the lead (warning) time each feature offers. Note that the fire spread rates are computed based on the Rothermel model and the shortest path algorithm is used to model fire growth in wildfire simulation. As shown in Fig. 5, the fire crosses the feature and the boundary of the residential area at time t_2 and t_3, respectively, and the lead time is computed as $t = t_3 - t_2$. Note that we assume that the fire spreads using the shortest path, and thus the lead time $t_3 - t_1$ the ETB(T) can provide should align with the input time T.

We use viewshed analysis to evaluate the prominence of the features and select prominent features as trigger points. Specifically, different application contexts are considered, as listed in Table 2. The viewpoint can be the location of a firefighter in the wildlands. In this case, LoS analysis can be performed to determine the visibility of the target feature from the viewpoint, as shown in Fig. 6(a). The second scenario is to determine the visibility of many features from one location. As shown in Fig. 6(b), the viewpoint is a firefighter or a group of firefighters' location, while the target represents a feature. Note that the result from viewshed analysis is a raster dataset in which visible and obscured cells are assigned with 1 and 0, respectively. We compute the raster cell each retrieved feature falls within to evaluate its visibility. Firefighters often use linear features (e.g. roads, trails, and fuel breaks) to travel between locations, provide evacuation routes, and control fire activity. Calculation of trigger points visibility from a polyline would help determine the utility of triggers for firefighters along one of these linear features. The third scenario uses a polyline to represent the firefighters' locations. The calculation of a cumulative viewshed can be considered as a combination of the viewshed of each viewpoint:

$$CV_{ij} = \sum_{k=1}^{n} V_{ij}^{k}$$

where CV_{ij} denotes the value of the raster cell at row i and column j in the cumulative viewshed, V_{ij}^{k} denotes the value of the raster cell located at row i and column j in the viewshed of the kth viewpoint, and n is the total number of viewpoints used in the cumulative viewshed calculation. Cumulative viewsheds depict the visibility of each raster cell from the vertices of the input polyline feature and can be used as a metric for feature prominence. The features located in the raster cells with larger values in the cumulative viewshed are more visible from the input firefighter locations than those with small values. For instance, as shown in Fig. 6(c), the input feature is a polyline, and its three vertexes are used to compute the cumulative viewshed. The raster cell value denotes the number of viewpoints from where the firefighters could see the cell. The features located within these dark green cells are more visible than these in the light green cells. Specifically, the feature in the dark green cell could be seen by firefighters located at the three viewpoints, while the two features in the light green cell could only be seen by firefighters located at one of the three viewpoints.

4. Case study

With a combination of flammable vegetation (e.g., chaparral), extreme weather conditions (Santa Ana winds), and extensive WUI, southern California has become one of the most vulnerable areas to wildfires in the U.S. The area chosen for the case study is located in Julian—a census-designated place (CDP) in the east of San Diego County, California. The 2003 Cedar fire occurred in this area and caused 26 fatalities and the loss of thousands of buildings. Specifically, the Julian downtown area and the Whispering Pines and

Table 2
Visibility analysis methods and their potential applications.

Analysis method	Potential application
Line of Sight (LoS) analysis	Can be used to calculate whether a firefighter or a group of firefighters at one location can see a specific feature.
Viewshed analysis	Can be used to calculate all the features a firefighter or a group of firefighters at one location can see.
Cumulative viewshed analysis	Can be used to calculate the visibility of the features to the firefighters at many locations (e.g., along a linear fuel break).

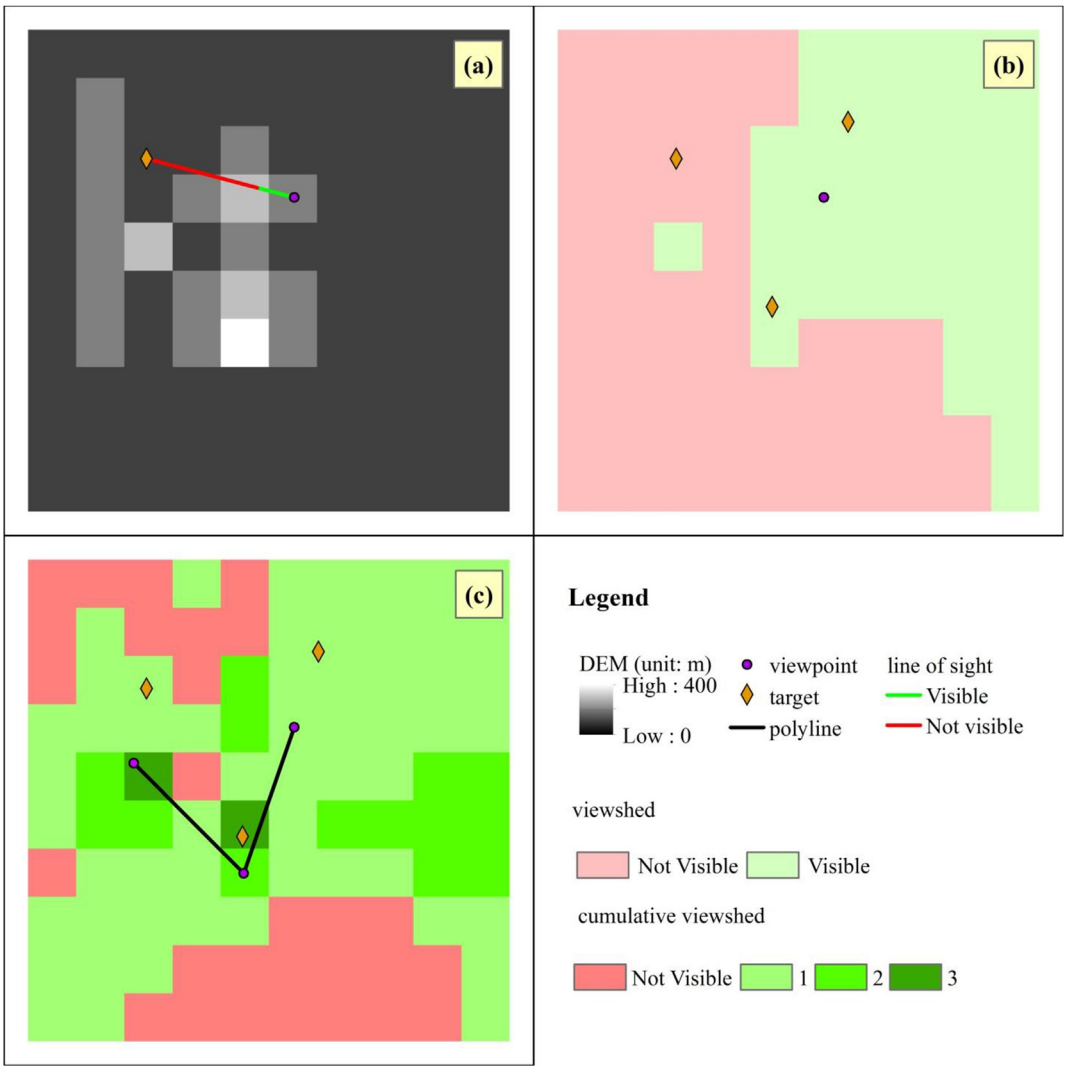

Fig. 6. Demonstration of LoS and viewshed analysis.

Kentwood communities were included as the threatened residential area in this case study. The selected residential area is surrounded by grass, shrub, and tree fuel types and can represent many fire-prone communities in the American West. As shown in Fig. 7, the residential area used as the input for trigger modeling is composed of raster cells. The administrative boundary dataset of Julian was acquired from the GIS department of San Diego County—SanGIS. The fuel, DEM, aspect, slope, and canopy cover data were downloaded from the LANDFIRE project, an open data portal that provides national datasets for various types of data used in wildfire-related studies in the U.S. (Rollins, 2009).

All the data acquired from LANDFIRE are at 30 m resolution, and the datasets include 1500 × 1500 raster cells and cover Julian and its surrounding area. Specifically, the fuel data in this study use the 13 Anderson fuel model (Anderson, 1982). Burnable fuel model 1 (short grass), 2 (timber), and 5 (brush) account for 58.4%, 22.6%, and 7.8%, respectively, while unburnable fuel model 91 (urban) and 99 (barren) are 2.7% and 4.2% respectively. These fuel models account for 95.8% of all raster cells. The environmental parameters listed in Table 3 were used as the input for fire spread modeling in FlamMap. We used this specific set of parameters to demonstrate the proposed method. In practice, environmental parameters would be based on local observed or predicted values. Note that larger fuel moisture values will reduce fire spread rates and generate a smaller trigger buffer, while a higher wind speed will usually increase the size of the generated trigger buffer along the wind direction.

The input ETE T for trigger modeling was set to 90 min, and Fig. 8(a) shows the derived 90 ETB and its boundary. Fig. 8(b) shows the retrieved features along the boundary of the 90 min ETB. Specifically, a total number of 1023 query points were employed to retrieve geographic features using the GeoNames online reverse geocoding service, and 28 unique features were derived. The 75 min and 105 min ETBs were also computed using trigger modeling, as shown in Fig. 8(c). A raster calculation operation was performed to subtract the 75 min ETB from the 105 min ETB to derive a selection space, and five features fall within this constructed selection space, as shown in Fig. 8(d).

The features derived from GeoNames include various types of natural and man-made features, such as a populated place, mine, school, park, reservoir, and stream. Note that the five features could be potentially used as trigger points to provide residents with between 75 and 105 min for their evacuation, assuming the actual fire's rate-of-spread (ROS) does not exceed the modeled ROS. Features that fall between the selection space and the residential area could be used as trigger points for an ETB generated using an evacuation time less than 75 min; and those falling out of the

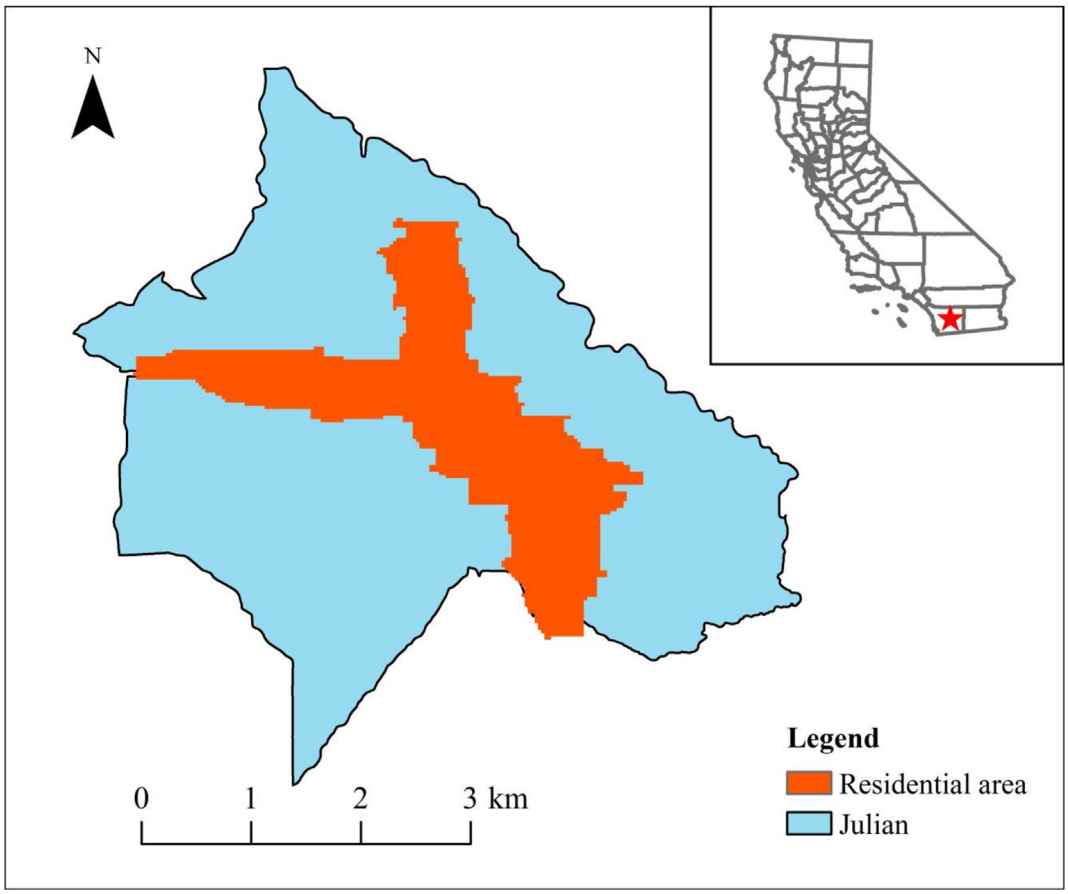

Fig. 7. Map of Julian, California.

Table 3
Environmental parameters for fire spread modeling.

Wind direction	Wind speed (km/h)	Dead fuel moisture (%)			Live fuel moisture (%)	
		1 h	10 h	100 h	Wood	Herbaceous
Northwest	16	5	5	5	65	65

selection space could be potentially used for an ETB derived using an input time greater than 105 min. Table 4 lists the five features in Fig. 8(d). Specifically, the GeoNames feature identification (ID), name, and feature class are included for each feature.

4.1. Feature prominence

We performed LoS and cumulative viewshed analysis for the feature named "Eastwood Creek" in Table 4. As shown in Fig. 9(a), the results of the LoS analysis indicate that when a feature is used as a trigger point, the nearby firefighters located at viewpoint 1, 4, and 5 could detect it when the fire crosses the feature. This could also help firefighters communicate with others about the whereabouts of the fire and facilitate evacuation warnings. Topographic obstructions exist between the target feature and viewpoint 2 and 3, and this feature cannot be seen by the firefighters located at these two locations. Note that this method does not take into account the obstacles (e.g., trees and buildings) between the firefighters and potential trigger points. We used an example of a hypothetical fuel break, represented as a polyline in Fig. 9(b), as the input for cumulative viewshed analysis. The polyline is comprised of a total of 106 vertexes, and the value of each raster cell in the cumulative viewshed map denotes the number of vertexes from which the cell could be seen. The value of the raster cell the feature falls within is 53, indicating that this feature could be seen from 53 out of 106 vertexes. A feature that falls within dark green cells is more visible than those in light green cells.

4.2. Spatial configuration and the timing of warnings

In order to demonstrate the potential use of a derived trigger point from GeoNames, we selected the Eastwood Creek as a trigger point for three wildfire scenarios, as shown in Fig. 10. Wildfire simulation was performed for each ignition point using the same environmental inputs listed in Table 3. The fire arrival and lead times for the ETBs and trigger point calculated using fire simulations are listed in Table 5. Fire arrival time contours were created to better illustrate the spatial relationships between fire perimeters and the trigger point as well as their impacts on evacuation timing, as shown in Fig. 11 (the numbers in Fig. 11(b), (d), and (f) denote fire travel times associated with the fire perimeters). In scenario 1 (Fig. 11(a) and (b)), the modeled fire reached the community before it crossed the trigger point, which implies that this feature was not useful for this scenario. In scenario 2 (Fig. 11(c)), when the fire crosses the trigger point, the residents should have about 70 min to evacuate before the fire reaches the community. In scenario 3 (Fig. 11(e) and (f)) the lead time when the fire crosses the trigger point is 42 min, which may lead to insufficient warning time to evacuate. Note that the trigger point is located to the east of the boundary of the 90 min ETB, which results in less lead time when it

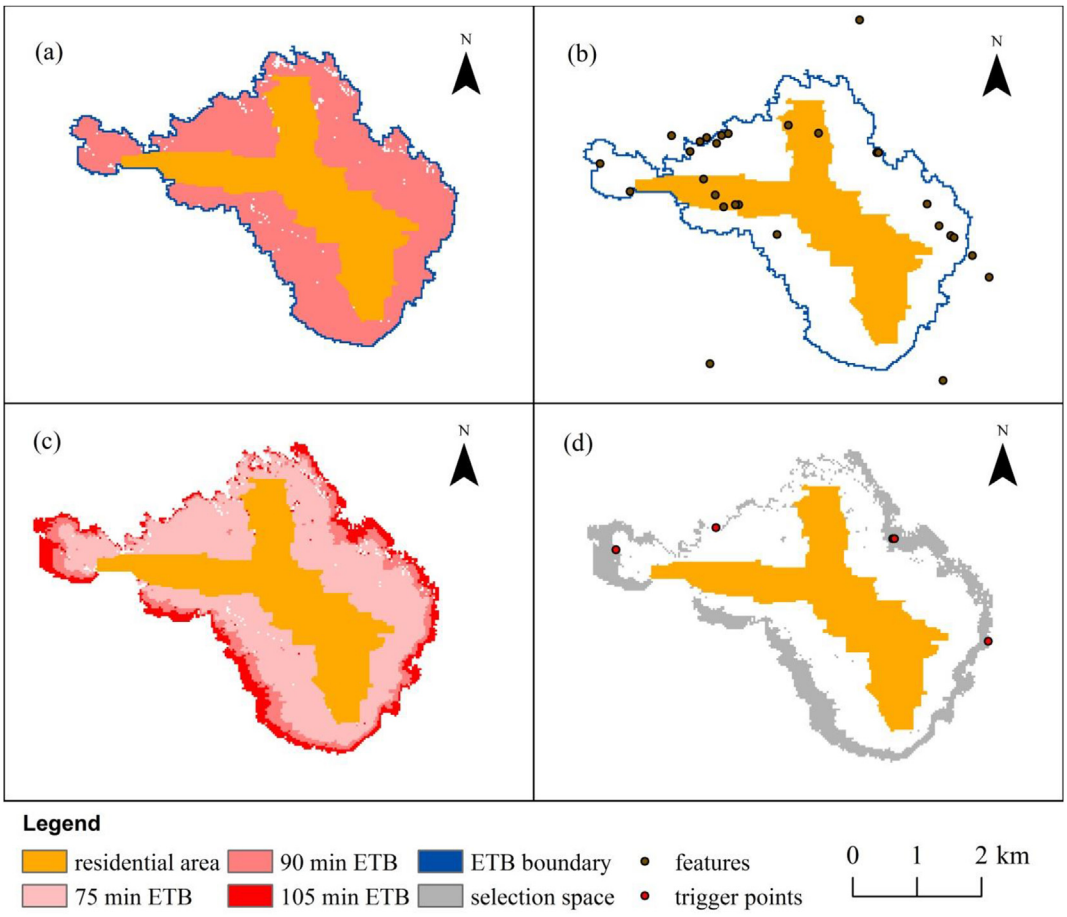

Fig. 8. Maps of ETBs and the retrieved geographic features.

is used to trigger an evacuation warning, as shown in a larger scale map of scenario 2 in Fig. 11(d). From the spatial configurations of fire perimeters, ETBs, and the trigger point, two findings emerge. First, a trigger point has more value when it is closer to the buffer boundary. Second, a trigger point has more value when it is closer to the fire front because wildfires can spread around a point feature that is far from a community. Another finding from the case study is that when retrieving features to set trigger points, we cannot simply reply on Euclidean distance between a trigger feature and a community because fire spread is rarely uniform. Thus, all computations should be conducted in a space characterized by fire travel times rather than a simple Euclidean space.

In order to further evaluate the value of the derived features, we also examined the timing of warnings of different features in one fire simulation scenario. Specifically, ignition point 1 and the same environmental inputs were used for the fire simulation. The lead time associated with each feature was calculated based on fire travel times, and Fig. 12 shows the derived lead times for the features. The lead times of the features located within the residential area all have negative values, which means that these features would not provide enough warning time for a successful evacuation. Note that there is a cluster of features located along the buffer boundary facing the fire front, and the lead times they provide vary significantly. For example, the outmost feature provides a lead time of 133 min, which is more time than that the original trigger buffer provides (90 min), while the innermost feature in this cluster has a negative lead time value −14 min, which means the fire will have reached the residential area before it crosses this feature.

Table 4
Retrieved geographic features from GeoNames.

GeoNamesID	Name	Feature class
5345692	El Dorado Mine	spot building farm
5346201	Ella Mine Group	spot building farm
5337485	Cimarron Elementary School	spot building farm
5345212	Eastwood Creek	stream lake
5363094	Keystone Pilot Mine	spot building farm

4.3. Geovisualizing lead time and visibility

In order to facilitate the use of these derived features as trigger points by the ICs in wildfire evacuation, both the lead time and the visibility information of these features were mapped in Fig. 13. This geovisualization could help the ICs more directly identify the features that can provide enough warning time and have good visibility and use them as trigger points. Note that the cumulative visibility value denotes the number of times the feature can be seen from the vertexes of the input polyline fuel break and is used as a preliminary metric for visibility evaluation in this context. For example, the features with 65 and 62 min lead times are more visible than the features with 9 min and 20 min lead times. The outmost feature can provide 133 min's warning time but is not visible from the fuel break. Thus, it cannot be used as an effective trigger point if the firefighters need to visually detect the fire's crossing the feature and use the feature in their communications.

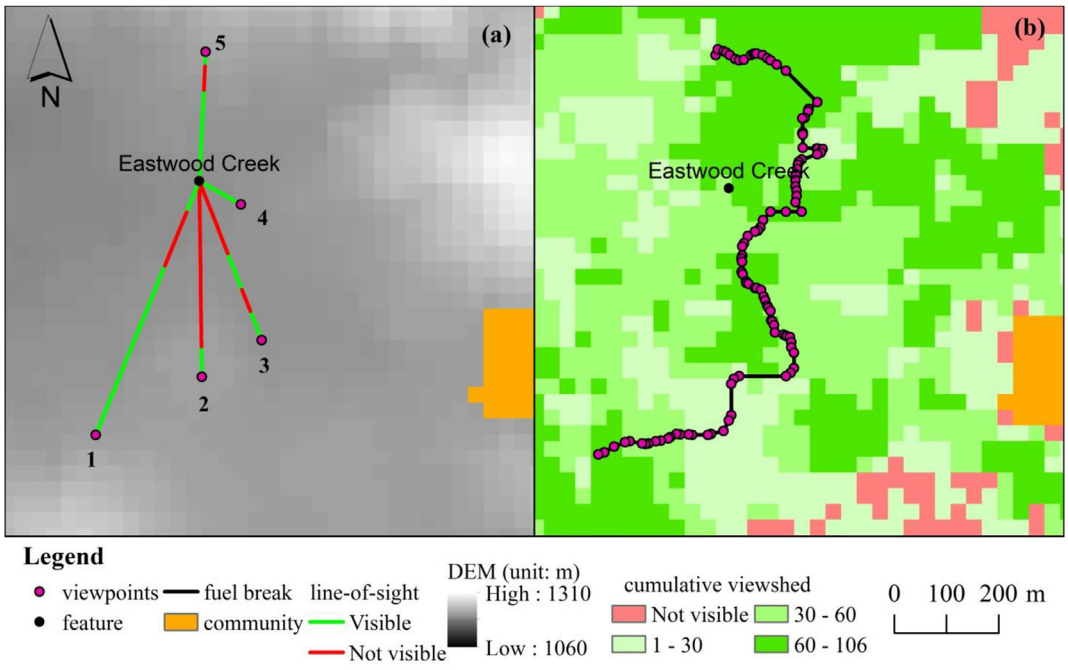

Fig. 9. Results of LoS and cumulative viewshed analysis.

5. Discussion

This work presents a method to identify and select prominent geographic features as trigger points. Specifically, this method accounts for both warning time and feature prominence during feature selection. The input time for trigger modeling is usually based on the time needed for the safe evacuation of the threatened population (Cova et al., 2005) and can be estimated by the incident

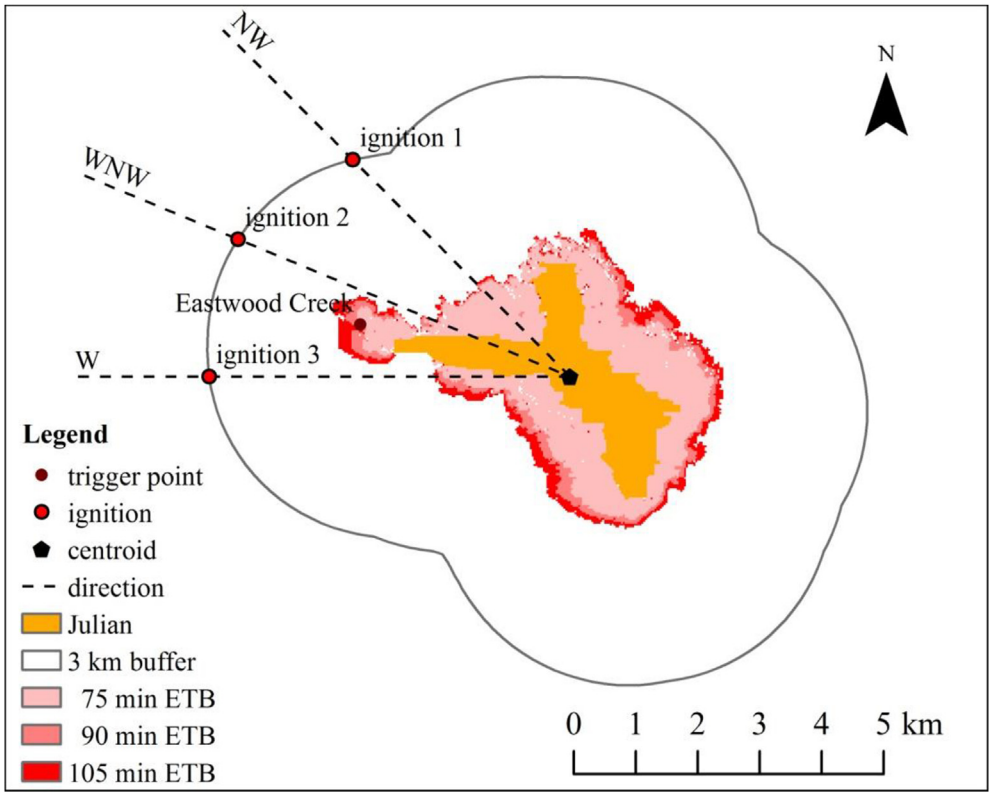

Fig. 10. Three scenarios for evaluating the method.

Table 5
Fire arrival and lead times calculated from wildfire simulations.

Fire arrival time (lead time) in min from			To location
Ignition 1	Ignition 2	Ignition 3	
420 (105)	239 (103)	239 (105)	105 min ETB
437 (88)	253 (89)	256 (88)	90 min ETB
458 (67)	269 (73)	270 (74)	75 min ETB
538 (−13)	272 (70)	302 (42)	Trigger point
525 (0)	342 (0)	344 (0)	Community

commander when the proposed method is used in practice. Note that trigger buffers generated using different input ETEs could be associated with different PARs (Cova et al., 2017). For example, if the input time is larger than the time needed by the residents or firefighters to evacuate to safe places, the generated trigger buffer could serve as an ETB; otherwise it could be associated with SIP. Thus, more work needs to be done to model the uncertainty in the input time. When estimating evacuation times for a threatened WUI community, traffic simulation could be employed to achieve the goal (Cova & Johnson, 2002; Wolshon & Marchive, 2007). Thus, evacuation traffic simulation could be performed to model the uncertainty in ETE from a statistical perspective, which will further improve trigger modeling. Moreover, this work uses viewshed analysis as a preliminary means to evaluate feature prominence. Note that other factors such as weather conditions, smoke, and obstacles could affect the visibility of the features, and these factors should be further examined to better evaluate feature visibility.

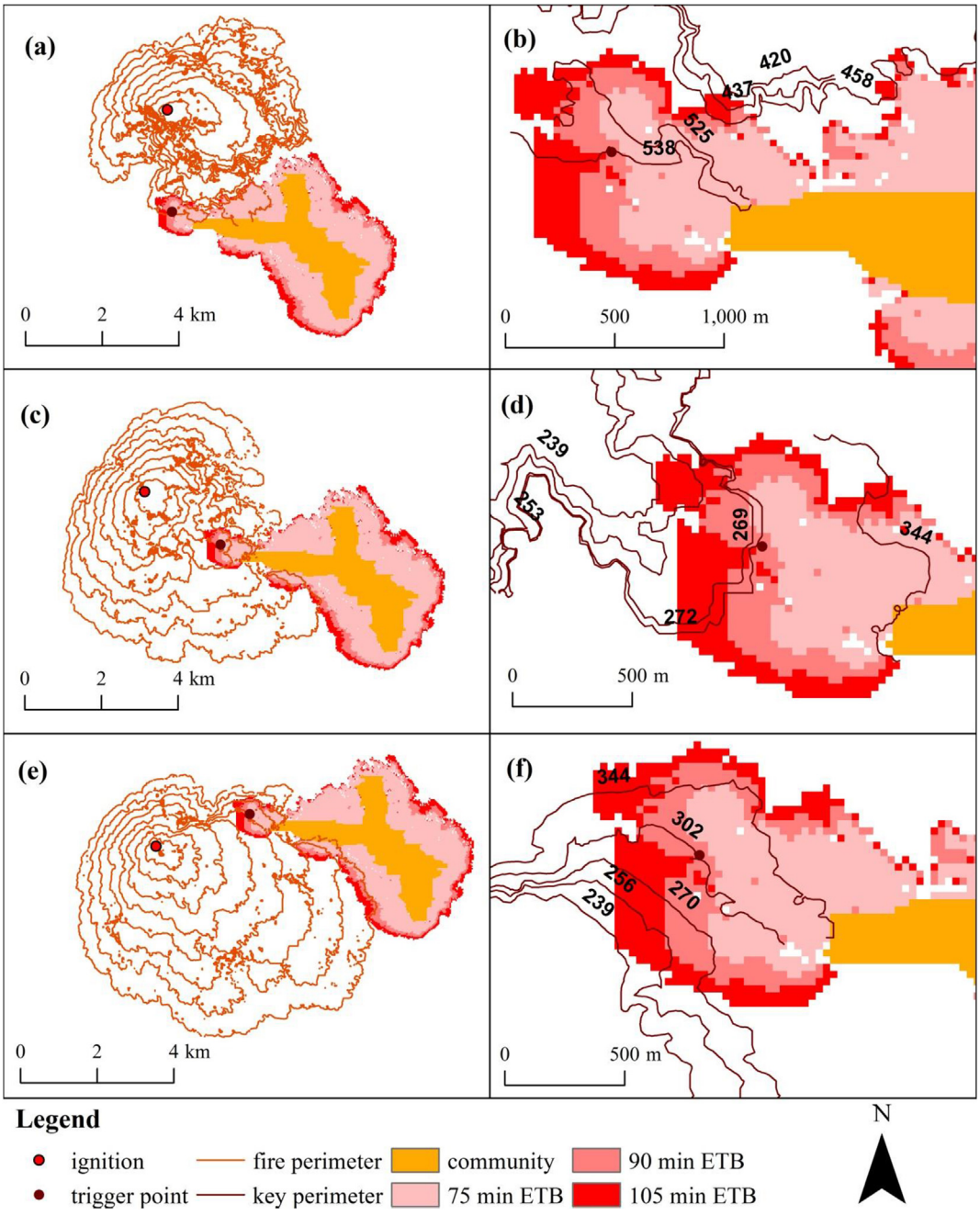

Fig. 11. Fire perimeters for the three scenarios.

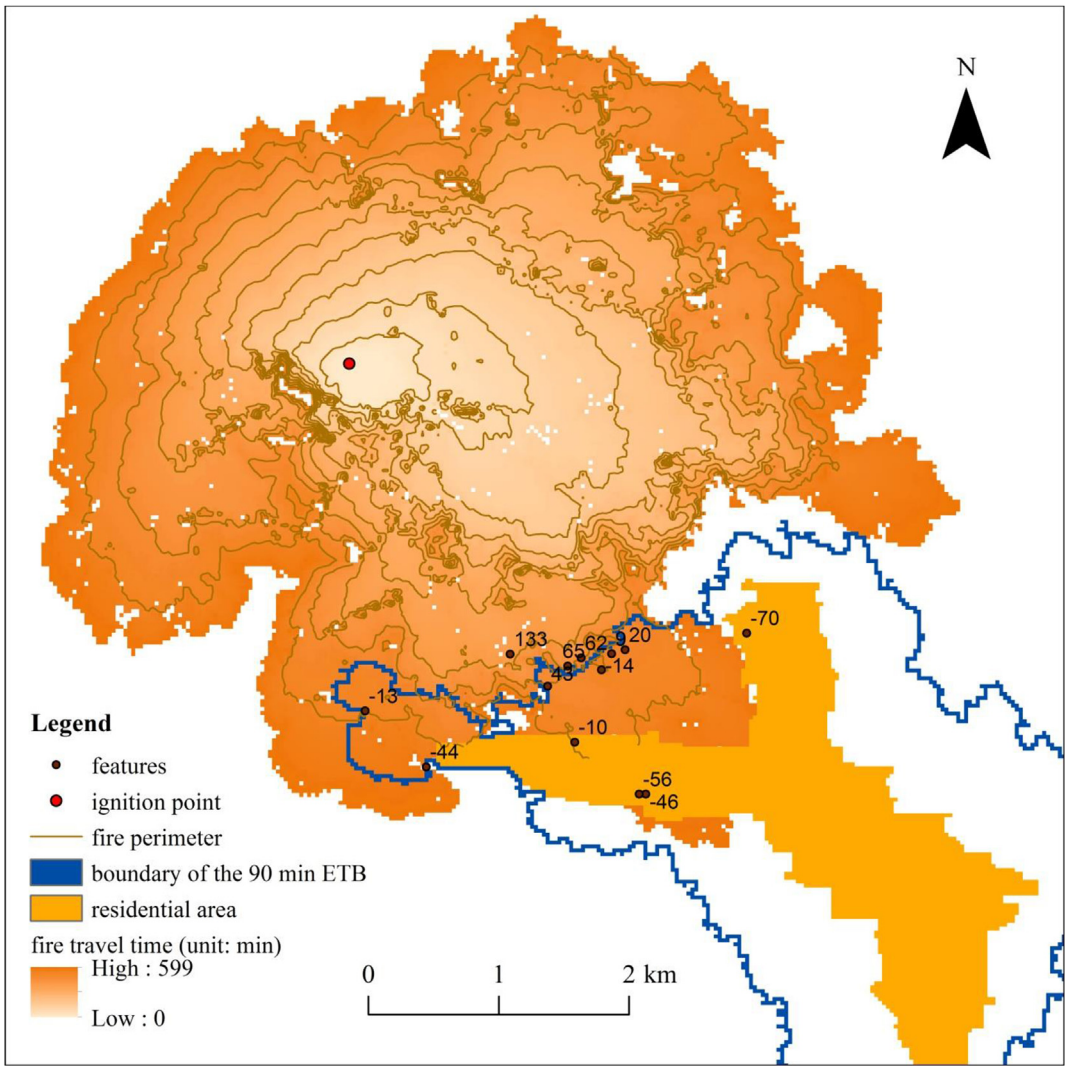

Fig. 12. Lead times calculated from fire simulation.

Furthermore, other characteristics such as the type, size, shape, color, and texture of the features as well as people's spatial perception and cognition could also be potential metrics for prominence evaluation, and more work should be conducted to explore feature prominence in the context of wildfire evacuation.

This work uses a publicly available online reverse geocoding service to retrieve geographic features around the boundary of the ETB. With the popularity of cloud computing, software as a service (SaaS) is being widely adopted in geospatial cyber-infrastructure (Yang, Raskin, Goodchild, & Gahegan, 2010; Yang et al., 2011). As noted, online reverse geocoding services can be integrated into various information systems with ease. However, the black-box characteristics of these online services pose challenges in various applications. For example, accuracy and privacy have been considered significant concerns for using online geocoding services in crime studies (Kounadi et al., 2013). In the context of trigger modeling, the accuracy of these online services is important, while privacy may not be a big concern. Specifically, the importance of the accuracy of these services lies in that the accuracy of the locations of the derived features that are used as trigger points could determine the evacuation timing for the residents at risk during wildfire evacuation. Thus, further study should be done to examine the accuracy of these online reverse geocoding services and its impact on wildfire evacuation timing to help develop a better understanding of them before they are used in real-world practice. We used GeoNames in reverse geocoding to demonstrate the potential use of the proposed method because this global gazetteer includes many types of natural and man-made geographic features. We also used Google's reverse geocoding service, and a total number of 100 distinct features were derived for 1023 input query points. The derived features from Google are street addresses or route names. These preliminary results reveal that GeoNames includes more feature types but its feature density is low and does not include many addresses and routes in the study area. Recent studies on the quality of digital gazetteers have analyzed the features types and the spatial distribution of the features (Acheson, De Sabbata, & Purves, 2017; Ahlers, 2013; Zhu, Hu, Janowicz, & McKenzie, 2016). However, these studies usually use open data to evaluate the general quality of the gazetteers and are not tailored for relevant exurban applications such as trigger modeling. Thus, another direction for future research is to perform a more comprehensive study on the types and spatial distribution of prominent geographic features from different reverse geocoding services in the WUI and its surrounding wildland area so as to evaluate the potential of using these features as trigger points in these areas.

The geographic features retrieved from online reverse

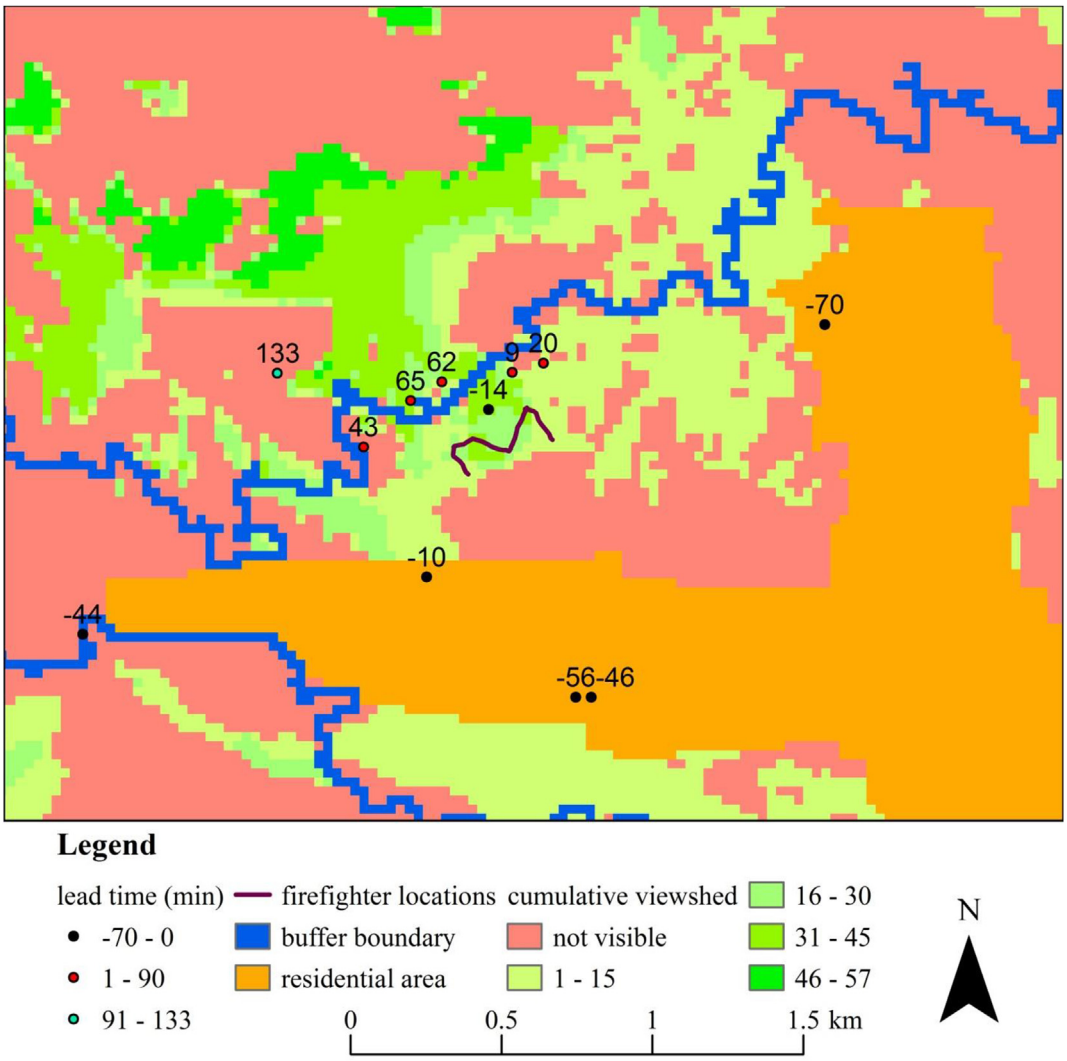

Fig. 13. Geovisualization of the lead time and visibility information of the features.

geocoding services are usually represented as geographic points. Note that a point can effectively represent small scale geographic features like a small building but cannot represent features like rivers and roads with an accepted level of accuracy. Thus, we also need to take into account spatial representation when using features as trigger points. The feature retrieved from GeoNames is a point feature, while Eastwood Creek should be represented as a polyline feature. Note that when a linear feature is used as a trigger point, its orientation and the spatial relationship between it and the fire perimeters also influence its effectiveness. It is also worth mentioning that the features that could be used as trigger points could be at a very fine scale and may not be readily available from existing data sources. A digital gazetteer is defined as a collection of geographic names with their footprints and descriptions (Goodchild & Hill, 2008; Hill, 2000). GeoNames is a global gazetteer, but the footprints of the features are points. As a matter of fact, in a typical digital gazetteer, the footprints of geographic features are no longer restricted to points but also can be represented using polylines and polygons. Thus, further research could be conducted to examine how to design and build a digital gazetteer to support trigger modeling. Specifically, the features derived from a gazetteer could be points, polylines, and polygons, which will involve more complex spatial analysis during the feature selection step. More efforts could be made in future work to compile detailed geographic data and build a special web service for trigger modeling.

6. Conclusion

The proposed method for identifying valuable trigger points provides a means of associating the buffers generated in trigger modeling with geographic features in the real world. In terms of key contributions, this work presents a computational method to incorporate online reverse geocoding into trigger modeling to identify geographic features, and the method can be integrated into various information systems for wildfire evacuation. Second, the method takes into account timing of warning and feature prominence during feature selection and uses wildfire simulation to examine evacuation timing. Third, a geovisualization method is proposed to present warning time and visibility information of the features, which could improve the ICs' and firefighters' situational awareness during wildfire evacuation. Lastly, the case study reveals that features located closer to buffer boundary and fire front may have more value when used as trigger points because the fire is less likely to skirt them. Also, prominent features may also have more value because they make it much easier for officials (or residents) to detect when the trigger event has occurred. The proposed method can be used for both setting trigger points long before any actual

fire occurs (strategic) and setting trigger points during a fire (operational) application. These methodological innovations and new findings supplement the existing trigger modeling method and make it more applicable in real-world evacuation scenarios. Future work can focus on above-mentioned aspects to develop a better understanding of using prominent geographic features to facilitate communications and navigation during wildfire evacuations.

Acknowledgment

This research was supported by National Science Foundation CMMI-IMEE grant number 1100890. We would like to thank the reviewers for their insightful comments and suggestions. We also thank the Center for High Performance Computing at the University of Utah for providing computing resources and technical support for our research.

References

Acheson, E., De Sabbata, S., & Purves, R. S. (2017). A quantitative analysis of global gazetteers: Patterns of coverage for common feature types. *Computers, Environment and Urban Systems, 64*, 309–320.

Ahlers, D. (2013). Assessment of the accuracy of GeoNames gazetteer data. In *Proceedings of the 7th workshop on geographic information retrieval* (pp. 74–81). New York, NY, USA: ACM GIR '13.

Anderson, H. E. (1982). *Aids to determining fuel models for estimating fire behavior*. Ogden, UT: USDA Forest Service, Intermountain Forest & Range Experiment Station.

Andresen, M. A. (2006). Crime measures and the spatial analysis of criminal activity. *British Journal of Criminology, 46*(2), 258–285.

Anguelova, Z., Stow, D. A., Kaiser, J., Dennison, P. E., & Cova, T. (2010). Integrating fire behavior and pedestrian mobility models to assess potential risk to humans from wildfires within the U.S.–Mexico border Zone*. *The Professional Geographer, 62*(2), 230–247.

Bonner, M. R., Han, D., Nie, J., Rogerson, P., Vena, J. E., & Freudenheim, Jo L. (2003). Positional accuracy of geocoded addresses in epidemiologic research. *Epidemiology, 14*(4), 408–412.

Brenkert–Smith, H., Champ, P. A., & Flores, N. (2006). Insights into wildfire mitigation decisions among wildland–urban interface residents. *Society and Natural Resources, 19*(8), 759–768.

Cook, R. (2003). Show low Arizona inferno: Evacuation lessons learned in the Rodeo-Chedeski fire. *National Fire Protection Association Journal, 97*(2), 10–14.

Cova, T. J., Dennison, P. E., & Drews, F. A. (2011). Modeling evacuate versus shelter-in-place decisions in wildfires. *Sustainability, 3*(12), 1662–1687.

Cova, T. J., Dennison, P. E., Kim, T. H., & Moritz, M. A. (2005). Setting wildfire evacuation trigger points using fire spread modeling and GIS. *Transactions in GIS, 9*(4), 603–617.

Cova, T. J., Dennison, P. E., Li, D., Drews, F. A., Siebeneck, L. K., & Lindell, M. K. (2017). Warning triggers in environmental hazards: Who should be warned to do what and when? *Risk Analysis, 37*(4), 601–611.

Cova, T. J., Drews, F. A., Siebeneck, L. K., & Musters, A. (2009). Protective actions in Wildfires: Evacuate or shelter-in-place? *Natural Hazards Review, 10*(4), 151–162.

Cova, T. J., & Johnson, J. P. (2002). Microsimulation of neighborhood evacuations in the urban–wildland interface. *Environment and Planning a, 34*(12), 2211–2229.

Davis, J. B. (1990). The wildland-urban interface: Paradise or battleground? *Journal of Forestry, 88*(1), 26–31.

Dennison, P. E., Brewer, S. C., Arnold, J. D., & Moritz, M. A. (2014). Large wildfire trends in the western United States, 1984-2011. *Geophysical Research Letters, 41*(8), 2928–2933.

Dennison, P. E., Cova, T. J., & Moritz, M. A. (2007). WUIVAC: A wildland-urban interface evacuation trigger model applied in strategic wildfire scenarios. *Natural Hazards, 41*(1), 181–199.

Dijkstra, E. W. (1959). A note on two problems in connexion with graphs. *Numerische Mathematik, 1*(1), 269–271.

Duckham, M., Kulik, L., & Worboys, M. (2003). Imprecise navigation. *GeoInformatica, 7*(2), 79–94.

Finney, M. A. (2006, March). An overview of FlamMap fire modeling capabilities. In P. L. Andrews, & B. W. Butler (Eds.), *Fuels management—how to measure Success: Conference proceedings* (pp. 213–220). Fort Collins, CO: USDA Forest Service, Rocky Mountain Research Station.

Fisher, P. F. (1993). Algorithm and implementation uncertainty in viewshed analysis. *International Journal of Geographical Information Systems, 7*(4), 331–347.

Fisher, P., Farrelly, C., Maddocks, A., & Ruggles, C. (1997). Spatial analysis of visible areas from the bronze age cairns of mull. *Journal of Archaeological Science, 24*(7), 581–592.

Fryer, G. K., Dennison, P. E., & Cova, T. J. (2013). Wildland firefighter entrapment avoidance: Modelling evacuation triggers. *International Journal of Wildland Fire, 22*(7), 883–893.

Goldberg, D. W., Wilson, J. P., & Knoblock, C. A. (2007). From text to geographic coordinates: The current state of geocoding. *URISA Journal, 19*(1), 33–46.

Goodchild, M. F., & Hill, L. L. (2008). Introduction to digital gazetteer research. *International Journal of Geographical Information Science, 22*(10), 1039–1044.

Hammer, R. B., Stewart, S. I., & Radeloff, V. C. (2009). Demographic trends, the wildland–urban interface, and wildfire management. *Society & Natural Resources, 22*(8), 777–782.

Hill, L. L. (2000). Core elements of digital gazetteers: placenames, categories, and footprints. In *Research and advanced technology for digital libraries* (pp. 280–290).

Karimi, H. A., Sharker, M. H., & Roongpiboonsopit, D. (2011). Geocoding Recommender: An algorithm to recommend optimal online geocoding services for applications. *Transactions in GIS, 15*(6), 869–886.

Kounadi, O., Lampoltshammer, T. J., Leitner, M., & Heistracher, T. (2013). Accuracy and privacy aspects in free online reverse geocoding services. *Cartography and Geographic Information Science, 40*(2), 140–153.

Krieger, N. (1992). Overcoming the absence of socioeconomic data in medical records: Validation and application of a census-based methodology. *American Journal of Public Health, 82*(5), 703–710.

Krieger, N., Chen, J. T., Waterman, P. D., Soobader, M., Subramanian, S., & Carson, R. (2002). Geocoding and monitoring of US socioeconomic inequalities in mortality and cancer incidence: Does the choice of area-based measure and geographic level matter? the public health disparities geocoding project. *American Journal of Epidemiology, 156*(5), 471–482.

Krumm, J. (2007). Inference attacks on location tracks. In A. LaMarca, M. Langheinrich, & K. N. Truong (Eds.), *Lecture notes in computer Science: Vol. 4480. Pervasive computing* (pp. 127–143). Berlin, Germany: Springer Berlin Heidelberg.

Larsen, J. C., Dennison, P. E., Cova, T. J., & Jones, C. (2011). Evaluating dynamic wildfire evacuation trigger buffers using the 2003 Cedar Fire. *Applied Geography, 31*(1), 12–19.

Lascala, E. A., Gerber, D., & Gruenewald, P. J. (2000). Demographic and environmental correlates of pedestrian injury collisions: A spatial analysis. *Accident Analysis & Prevention, 32*(5), 651–658.

Li, D., Cova, T. J., & Dennison, P. E. (2015). A household-level approach to staging wildfire evacuation warnings using trigger modeling. *Computers, Environment and Urban Systems, 54*, 56–67.

Llobera, M. (2003). Extending GIS-based visual analysis: The concept of visualscapes. *International Journal of Geographical Information Science, 17*(1), 25–48.

Loo, B. P. Y. (2006). Validating crash locations for quantitative spatial analysis: A GIS-based approach. *Accident Analysis & Prevention, 38*(5), 879–886.

McKenzie, G., & Janowicz, K. (2015). Where is also about time: A location-distortion model to improve reverse geocoding using behavior-driven temporal semantic signatures. *Computers, Environment and Urban Systems, 54*, 1–13.

Mell, W. E., Manzello, S. L., Maranghides, A., Butry, D., & Rehm, R. G. (2010). The wildland–urban interface fire problem–current approaches and research needs. *International Journal of Wildland Fire, 19*(2), 238–251.

Millonig, A., & Schechtner, K. (2007). Developing landmark-based pedestrian-navigation systems. *IEEE Transactions on Intelligent Transportation Systems, 8*(1), 43–49.

Radeloff, V. C., Hammer, R. B., Stewart, S. I., Fried, J. S., Holcomb, S. S., & McKeefry, J. F. (2005). The wildland-urban interface in the United States. *Ecological Applications, 15*(3), 799–805.

Ratcliffe, J. H. (2004). Geocoding crime and a first estimate of a minimum acceptable hit rate. *International Journal of Geographical Information Science, 18*(1), 61–72.

Rollins, M. G. (2009). LANDFIRE: A nationally consistent vegetation, wildland fire, and fuel assessment. *International Journal of Wildland Fire, 18*(3), 235–249.

Roongpiboonsopit, D., & Karimi, H. A. (2010). Comparative evaluation and analysis of online geocoding services. *International Journal of Geographical Information Science, 24*(7), 1081–1100.

Rothermel, R. C. (1972). *A mathematical model for predicting fire spread in wildland fuels*. Ogden, UT: USDA Forest Service, Intermountain Forest & Range Experiment Station.

Rushton, G., Armstrong, M. P., Gittler, J., Greene, B. R., Pavlik, C. E., West, M. M., et al. (2006). Geocoding in cancer research: A review. *American Journal of Preventive Medicine, 30*(2), S16–S24.

Stewart, S. I., Radeloff, V. C., Hammer, R. B., & Hawbaker, T. J. (2007). Defining the wildland–urban interface. *Journal of Forestry, 105*(4), 201–207.

Theobald, D. M., & Romme, W. H. (2007). Expansion of the US wildland–urban interface. *Landscape and Urban Planning, 83*(4), 340–354.

Wolshon, B., & Marchive, E. (2007). Emergency planning in the urban-wildland interface: Subdivision-level analysis of wildfire evacuations. *Journal of Urban Planning and Development, 133*(1), 73–81.

Yang, C., Goodchild, M., Huang, Q., Nebert, D., Raskin, R., Xu, Y., … Fay, D. (2011). Spatial cloud computing: How can the geospatial sciences use and help shape cloud computing? *International Journal of Digital Earth, 4*(4), 305–329.

Yang, C., Raskin, R., Goodchild, M., & Gahegan, M. (2010). Geospatial Cyberinfrastructure: Past, present and future. *Computers, Environment and Urban Systems, 34*(4), 264–277.

Zandbergen, P. A. (2009). Geocoding quality and implications for spatial analysis. *Geography Compass, 3*(2), 647–680.

Zandbergen, P. A. (2011). Influence of street reference data on geocoding quality. *Geocarto International, 26*(1), 35–47.

Zandbergen, P. A., Hart, T. C., Lenzer, K. E., & Camponovo, M. E. (2012). Error

propagation models to examine the effects of geocoding quality on spatial analysis of individual-level datasets. *Spatial and Spatio-temporal Epidemiology, 3*(1), 69–82.
Zhu, R., Hu, Y., Janowicz, K., & McKenzie, G. (2016). Spatial signatures for geographic feature types: Examining gazetteer ontologies using spatial statistics. *Transactions in GIS, 20*(3), 333–355.
Zhu, R., & Karimi, H. A. (2015). Automatic selection of landmarks for navigation guidance. *Transactions in GIS, 19*(2), 247–261.